A MATHEMATICAL MODEL FOR STUDYING THE REACTION OF AN AIRCRAFT ENGINE BLADE TO A BIRD STRIKE

Dilshod Eshmuradov Elmuradovich[1], Seungjik Lee[2], Behzod Zhumamuratov Akramjonovich[3], Temurmalik Elmuradov Dilshod_o`g`li[4]

[1]*Head of the Department of "Energy Supply Systems" of the Tashkent University of Information Technologies, Candidate of Technical Sciences, Associate Professor, Academician of the Academy of Sciences of Turon*

[2]Ph.D, *Professor of the Department of "Artificial Intelligence" of the Tashkent University of Information Technologies*

[3]*doctoral student of the Department of "Metrology, technical regulation, standardization and certification" of Tashkent State Technical University named after Islam Karimov*

[4]*Senior Lecturer of Tashkent State Technical University named after Islam Karimov*

https://doi.org/10.5281/zenodo.10471056

Abstract. The method of studying the reaction of an aircraft engine blade to a bird strike is considered. A model of the contact interaction of a soft body with the blade of an aircraft engine has been developed. By comparing the results and mathematical modeling with the results of the experiment, the efficiency and operability of the proposed model and method for studying the bird resistance of aircraft engine blades are proved.

Keywords: aircraft engine, blade, bird, impact, stability.

INTRODUCTION

Cases of birds getting into an aircraft engine raise a number of questions related to the reliability of aircraft equipment and flight safety. The annual cost of bird strikes to commercial aircraft worldwide is estimated at US $1.3 billion. Considering that in the coming years the likelihood of solving the problem of eliminating cases of birds entering an engine during operation is very low, one of the effective ways to reduce the negative impact of birds and improve operational quality and flight safety is to create engines that are resistant to damage resulting from these collisions. In birds, the durability of aircraft engines is assessed using mathematical modeling methods and experimentally. One of the reasons for the high cost of developing an aircraft engine is the fact that the design process involves the need for expensive full-scale testing. One of the effective ways to reduce the cost of engine development is to reduce the number of full-scale tests and partially replace them with numerical experiments. In addition to reducing cost, the use of a computational experiment can reduce development time by 3 times and improve the quality of the finished product. Therefore, the development of numerical models of contact interaction between a bird (soft body) and an aircraft engine blade (obstacle) with the aim of introducing them into the practice of designing bird-resistant blades is an urgent scientific and technical problem.

The goal of the work is to develop a mathematical model of the interaction of a soft body with an aircraft engine blade and a method for studying its response to impact.

The process of a soft body colliding with an obstacle is a complex physical and mechanical process, with its inherent features and certain methodological difficulties associated with its modeling. The problem of a collision of a soft body with an obstacle is a non-stationary, spatial, contact problem of continuum mechanics. Figure 1 shows a block diagram of the computational and experimental method for studying the mechanical processes of contact of a soft body with an engine blade.

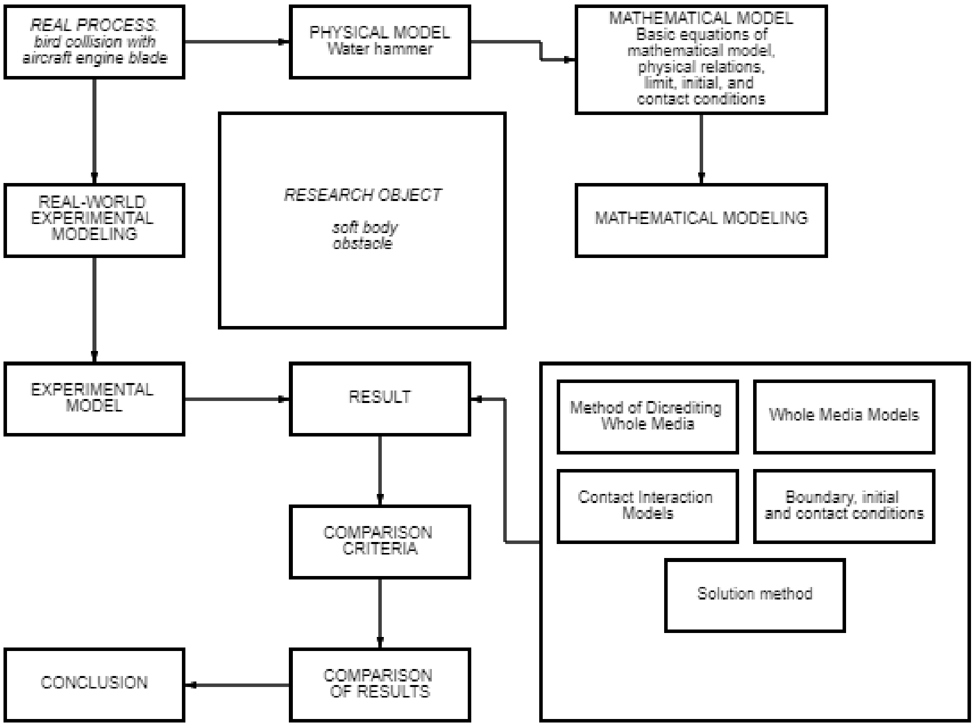

Figure 1 - Computational and experimental method for studying the mechanical processes of contact of a soft body with an engine blade

The practical implementation of the method under consideration involves a consistent transition from a real phenomenon to an idealized representation. It has the form of continuous media in order to obtain qualitative and quantitative results from numerical simulation of a real phenomenon. The physical model describes the phenomenon of water hammer [1], which accompanies the collision process. There are four stages of water hammer: 1) active (initial), which is associated with the propagation of the shock wave; 2) the stage of pressure decline, which is accompanied by the propagation of a rarefaction wave; 3) stage of steady flow and 4) termination of the process. A mathematical model, represented by a system of partial differential equations, describes the mechanical motion and thermo mechanical state of deformable bodies. Together with geometric and physical relationships, as well as limit, initial and contact conditions, the equations of the mathematical model constitute a general initial-boundary value problem.

The construction of a numerical model involves the transition from differential equations (strong form) to the integral equation of motion (weak form) through the variational principle of virtual works. Within the framework of this stage, the following problems were solved: 1) the method of sampling the soft body and shoulder blade was chosen; 2) the effect of the sampling step on the accuracy of the resulting solution was investigated; 3) the influence of the shape of the soft body on the pressure distribution was investigated; 4) models of continuous media are selected; 5) a contact interaction model is selected and described; 6) the solution method is selected.

In order to verify the numerical model of contact interaction of the soft body with the blade and substantiate the reliability of the obtained results, the results of numerical modeling were compared with the results of a full-scale experiment. Comparison criteria were developed: qualitative and quantitative comparison using integral indicators and by the distribution of physical parameters.

PHYSICAL MODEL

The physical model was built with the following assumptions in mind:

1) the soft body is a cylinder having a length to diameter ratio of 2; *2)* soft body material is considered homogeneous; *3)* the strength of the soft body is small compared to the strength of the blade, and it is neglected; *4)* given the assumption specified in claim 3, there is no rebound of the soft body; *5)* forces of viscous damping in the material and friction forces on the contact surface are neglected; *6)* flow in the material beyond the shock wave front is one-dimensional, adiabatic and irreversible.

Figure 2 shows the four phases of the impact. The first phase-active (Fig. 2a) is characterized by a sharp increase in pressure due to sharp braking of particles in the zone of contact of the soft body with the obstacle and is associated with the propagation of the shock wave in the direction opposite to movement. The active phase of the impact is described using two parameters: Hugoniot pressure and pressure build-up time. The Hugoniot pressure [1] is defined according to the expression (1):

$$p_H = p_2 - p_1 = \rho_1 v_s v_0 \quad (1)$$

p_1 and p_2- pressure before and behind the shock wave front; v - the rate of propagation of the shock wave in the medium; v_0- impact speed.

The second phase-propagation of the vacuum wave (Fig. 2 b) is associated with the propagation of the vacuum wave from the free surface of the soft body to the center due to the formation of a zone of high pressure gradients. This in turn causes the free surface of the soft body to move radially relative to the obstacle. When the vacuum wave reaches the center of the soft body (point c, Fig. 2 b), a decrease in pressure is observed. The law of distribution of pressure (2) along the radius of the cylindrical volume is determined by the ratio [1]:

$$p_r = p_{\text{H}} e^{\frac{-kr}{R(t)}} \tag{2}$$

k-constant; an r-radius vector determining the location of the point at which the pressure is measured; R (t) is the maximum contact radius at time t.

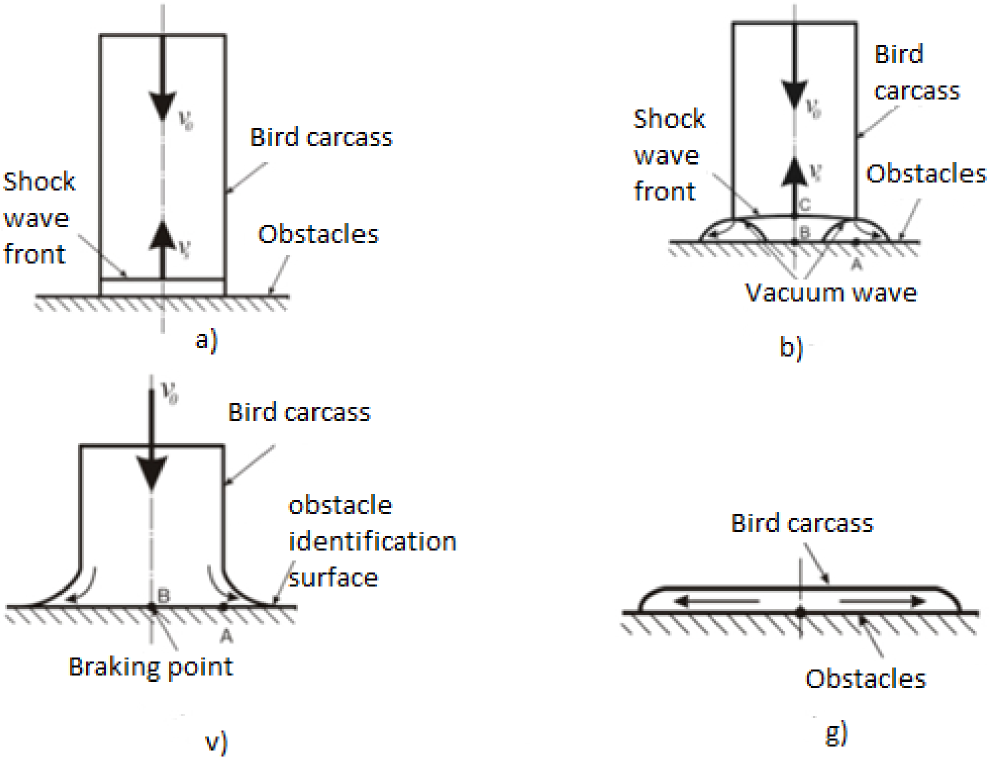

Figure 2 - Impact phases

In the third phase of steady-state flow (Fig. 2 v) - there is a decrease in radial pressures in the soft body and the occurrence of tangential stresses. Since the strength of the soft body under the action of tangential stresses is low, it spreads over the surface of the obstacle. At this stage, stationary pressure and velocity fields occur in the soft body. Braking pressure [1] at the central point "c" is estimated using expression (3):

$$p_s = \frac{1}{2}\rho_0 v_0^2 \tag{3}$$

ρ_0- density of soft body material at zero porosity.

In the fourth phase, as the upper free surface of the soft body approaches the obstacle, the speed of its movement decreases and the pressure increases. The pressure field is non-stationary and reaches the maximum value at the braking point, with subsequent reduction to atmospheric value as it moves away from the center. As the free surface of the soft body is in this pressure field, an instantaneous pressure drop occurs and the flow process stops (Fig. 2 g).

The duration of the impact process [1] can be estimated using expression (4):

$$t_D = {}^{L}\!/_{v_0} \tag{4}$$

L - is the length of the soft body.

MATHEMATICAL MODEL

The system of equations describing the motion and thermo mechanical state of deformable solid media is recorded in the actual configuration, and their differentiation and integration is carried out according to Euler coordinates.

$$\rho V = \rho_0, X \in V_T \cup V_b \tag{5}$$

ρ and ρ_0 - density of the medium at the current and initial time, respectively; $V = J = \det(F)$ - relative volume; V_T - part of the space of a given volume occupied by an obstacle; V_b - part of the space of a given volume occupied by a soft body.

$$\rho\frac{dv}{dt} = div\sigma, X \in V_T \cup V_b \tag{6}$$

$$\rho\frac{de}{dt} V s_{ij}\varepsilon_{ij} - (\rho + q)\dot{V},\ X \in V_T \cup V_b \tag{7}$$

v - velocity vector; $\frac{de}{dt}$ - acceleration vector; $div\sigma = \nabla \cdot \sigma$ - voltage tensor divergence;

$\nabla = \frac{\partial(\dots)}{\partial x} i + \frac{\partial(\dots)}{\partial y} j + \frac{\partial(\dots)}{\partial z} k$- Hamilton operator (Nabl operator); σ - Cauchy stress tensor; e - specific internal energy; ε - strain velocity tensor; p - pressure; q - volume viscosity; s_{ij} - components of the voltage deviator.

System of equations (5-7) is supplemented with kinematic (8) and geometric (9), (10) relations.

$$\frac{du}{dt} = v,\ X \in V_T \cup V_b \tag{8}$$

u - vector of movements.

$$\varepsilon_{ij} = \frac{1}{2}\left(\frac{\partial u_i}{\partial x_j} + \frac{\partial u_j}{\partial x_i} + \frac{\partial u_k}{\partial x_i}\frac{\partial u_k}{\partial x_j}\right); \tag{9}$$

$$\dot{\varepsilon}_{ij} = \frac{1}{2}\left(\frac{\partial v_i}{\partial x_j} + \frac{\partial v_j}{\partial x_i}\right) \tag{10}$$

Physical relations (11-13) describe peculiarities of behavior of deformable media manifested in the form of deformation resistance.

In the case of elastic-plastic behavior of the interference material, the components of the stress tensor are as follows:

$$p = K\left(\frac{1}{V} - 1\right); \tag{11}$$

$$s_{ij}^{\nabla} + 2G\dot{\Lambda} s_{ij} = 2G(\dot{\varepsilon}_{ij} - \dot{\varepsilon}_k g_{ij}); \tag{12}$$

K - bulk compression modulus; s_{ij} - derivative of voltage deviator; G- rigidity modulus; λ- scalar parameter; g_{ij} - metric tensor components.

To build a numerical method for solving a system of defining equations of a mathematical model, the variation principle of virtual works is used.

For the sampling of the soft body, the Smoothed Particle Hydrodynamics was used, which uses the Lagrangian approach to describe the movement of the continuous medium [2, p. 637-642; 3; 4]. The solid medium is represented by a discrete set of mobile particles that allow arbitrary connectivity with each other. Each of the particles is an interpolation point at which the media properties are set. The particle is defined by the spatial coordinates *xi(t)* and the mass *mt(t)*. The properties of the particle are determined by the smoothing length *(h)* using the kernel function *(W)*. The particle property A at an arbitrary point r is determined by summing the corresponding values of all particles within two smoothing lengths:

$$A(r_i) = \sum_{j=1}^{N} m_j \frac{A_j}{\rho_j} W\big((r_i - r_j), h\big);$$

m_j- mass of the j^th^ particle; A_j- value of parameter A of the j^th^ particle; ρ_j - density of the j^th^ particle; r-coordinate; h - smoothing length; *W*- weight function or core; *N* - number of adjacent to j^th^ particles.

The kernel function is defined by the anti-aliasing function in *θ (x):*

$$W(x,h) = \frac{1}{h(x)^d}\theta(x);$$

d- parameter that determines the dimension of the space, $x = r/h$

$$\theta(x) = \frac{1}{\pi h^3}\begin{cases} 1 - \frac{3}{2}\left(\frac{r}{h}\right)^2 + \frac{3}{4}\left(\frac{r}{h}\right)^3; & 0 \le \frac{r}{h} \le 1 \\ \frac{1}{4}\left(2 - \frac{r}{h}\right)^3; & 1 \le \frac{r}{h} \le 2 \\ 0; & \frac{r}{h} > 2 \end{cases};$$

After sampling, the main equations of the mathematical model take the form (13-14):

$$\rho_i = \sum_{j=1}^{N} m_j W_{ij}; \tag{13}$$

$$\frac{dv_i^{\alpha}}{dt} = \sum_{j=1}^{N} m_j\left(\frac{\sigma_i^{\alpha\beta}}{\rho_i^2} + \frac{\sigma_j^{\alpha\beta}}{\rho_j^2}\right)\nabla W_{ij}; \tag{14}$$

To sample the equation of motion in time, a modification of the method of central differences was used, which is implemented in the form of an explicit scheme of the 2^nd^ order with variable time increments [2, c. 501]. To find the solution to equation (21), the processing time is divided into nrs time intervals or steps in Δt time, where *n = 1...nTs*. Vector of nodal accelerations (15) on the n^{th} time layer is determined as a result of the rotation of the mass matrix:

$$\alpha^n = M^{-1}(f_{int}(u^n, t^n) + H^n); \tag{15}$$

The finite difference expression for determining the velocity vector on a half-integer time layer is (16):

$$v^{n+\frac{1}{2}} = v^{n-\frac{1}{2}} + \Delta t^n \alpha^n; \tag{16}$$

The finite difference expression for determining the node motion vector on the following time layer *tn + 1* is (17):

$$u^{n+1} = u^n + \Delta t^{n+\frac{1}{2}} v^{n+\frac{1}{2}}; \tag{17}$$

The updated position of the nodes is obtained by adding to the initial position vector the values of nodal movements calculated on the following time layer (18):

$$x^{n+1} = x^0 + u^{n+1}. \tag{18}$$

THE RESULTS OF THE RESEARCH

Using the method considered in the work and the constructed mathematical model of the contact interaction of a soft body with a blade of an aircraft engine, numerical studies of the reaction of a titanium alloy blade to the impact of a soft body of different weights, at different speeds and at different angles were carried out. Figure 3 shows the pattern of deformation of the soft body and blade during the first 250 μs for the case of an oblique impact of an 82.6 g soft body at a speed of 302.1 m/s at an angle of 36.4 ° to a cantilevered titanium alloy blade, which has the following dimensions: length 311.2 mm, width 88.9 mm and thickness 4.27 mm. The point of impact of the soft body on the blade is located at a distance of 70% of the blade span.

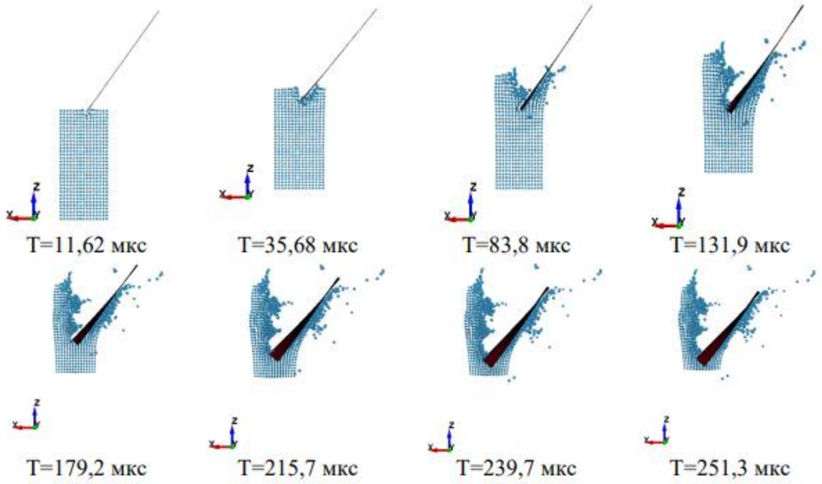

Figure 3 - Deformation pattern of soft body and blade in case of oblique impact

The obtained result makes it possible to analyze the trajectories of movement of particles of the soft body and to estimate the size and nature of probable damage to the blade. In the case of an oblique impact of a soft body on the blade, the soft body is divides into two parts, one of which interacts with the surface of the blade, and the other moves in the initial direction.

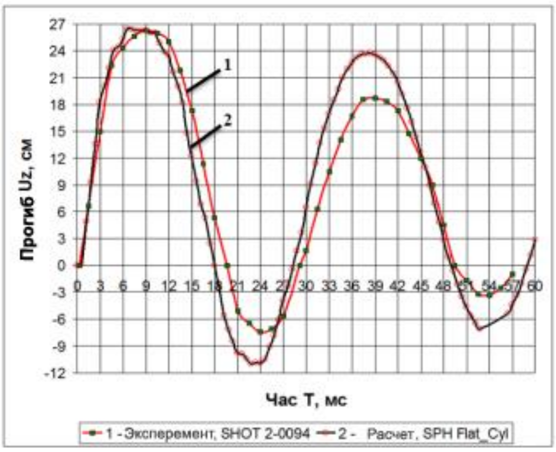

Figure 4 - Graph of the change in the dynamic deflection of the blade in the final section at frontal impact

Figure 4 shows a graph of the change in the dynamic deflection of the blade in the final section in the event of a frontal impact of a soft body weighing 100.5 g at a speed of 177.4 m/s along a cantilevered titanium alloy blade. Figure 5 shows the result of comparing the bending stresses in the root section of the blade for frontal and oblique impacts. The influence of the speed and angle of collision on the distribution of stresses in the root section of the blade was investigated.

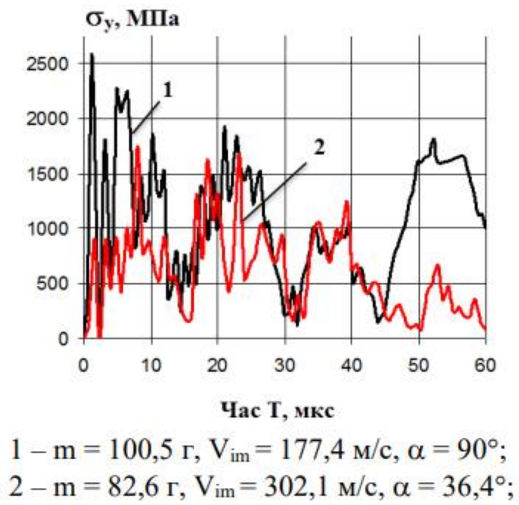

Figure 5 - Impact of impact process parameters on the distribution of normal stresses in the root section of the blade

When analyzing the distribution of normal stresses at the root intersection of the blade for both impact cases, the following should be noted: In terms of the probability of damage, the case of frontal impact is more dangerous than the case of oblique impact. Although in the case of oblique impact, the speed of the soft body is higher than in the case of frontal impact, the stress level for this case is lower than the corresponding stress level in the case of frontal impact. This indicates a more significant impact of the collision angle on the stress level than the speed. For both cases, the stress level exceeds the yield strength, as evidenced by the development of plastic deformations in the root section of the blade.

CONCLUSION

1. A hybrid model of the contact interaction of a soft body with an aircraft engine blade has been developed, which combines two sampling methods: the finite element method for a blade and the mesh-free method of smoothed particles for a soft body.

2. The use of a grid-free method of smoothed particles to sample a soft body eliminated problems of numerical instability and expanded the field of

modeling and investigation of mechanical processes accompanying impact.

3. Qualitative coordination of the results of numerical modeling with the results of a full-scale experiment, indicating the operability of the proposed model and the possibility of using it as an alternative to full-scale tests, was obtained. This, in turn, simplifies, accelerates, and reduces the material cost of designing new bird-resistant blades.

4. The use of first-order shell elements in a numerical model with a single integration point for sampling the blade reduces the computational cost compared to elements that use a complete integration scheme, and this in turn increases the computational efficiency of the model.

5. The model allows you to analyze the possible consequences of a soft body impact on the blade, assess the size and type of probable damage, as well as obtain a distribution of parameters characterizing the thermo mechanical state of the blade in time, as well as in volume.

REFERENCES

1. Impact Behavior of Low Strength Projectiles: Technical report / University of Dayton Research Institute; Wilbeck J. S. - 1978. - 129 p.
2. Hallquist J. O. LS-DYNA. Theory Manual. - Livermore: LSTC, 2006. - 680 p.
3. Monaghan J. J. Smoothed Particle Hydrodynamics [Электронный ресурс]. - URL: http://www.astro.lu.se/~Дэвид/учитель/SPH/заметки/ annurev.aa.30.090192.pdf.
4. Monaghan J. J. Smoothed Particle Hydrodynamics [Электронный ресурс]. - URL: http://cg.informatik.unifreiburg.de/intern/seminar / particleFluids_Monaghan%20-% 20sph % 20-% 202005.pdf.
5. Эшмурадов Д. Э., Элмурадов Т. Д., Саидрасулова Х. Б. АНАЛИЗ ЭКОНОМИЧЕСКОЙ ЭФФЕКТИВНОСТИ, ОБУСЛОВЛЕННОЙ ВНЕДРЕНИЕМ ЗОНАЛЬНОЙ НАВИГАЦИИ В РЕСПУБЛИКЕ УЗБЕКИСТАН //Актуальные аспекты развития воздушного транспорта (Авиатранс-2018). – 2018. – С. 88-92.
6. Эшмурадов Д. Э., Элмурадов Т. Д. МАТЕМАТИЧЕСКОЕ МОДЕЛИРОВАНИЕ АВИАЦИОННОЙ СРЕДЫ //Научный вестник Московского государственного технического университета гражданской авиации. – 2020. – Т. 23. – №. 5. – С. 67-75.
7. Ismailov O. Interaction of International Investment and Trade Regimes on Interpreting Treaty Necessity Clauses: Convergence or Divergence //Geo. J. Int'l L. – 2016. – Т. 48. – С. 505.